HETEROCYCLES, Vol. 104, No. 4, 2022, pp. 786 - 796. © 2022 The Japan Institute of Heterocyclic Chemistry
Received, 4th December, 2021, Accepted, 13th January, 2022, Published online, 21st January, 2022
DOI: 10.3987/COM-21-14603

SYNTHESIS OF AMIDE-FUNCTIONALIZED THIA[7]HELICENE-LIKE MOLECULE AND ITS SUPRAMOLECULAR ASSEMBLY IN THE SOLID STATE

Takumi Inoue,[a] Shohei Hamada,[a] Rina Nakamura,[a] Yusuke Kobayashi,[a] Takahiro Sasamori,[b] and Takumi Furuta[a]*

[a]Department of Pharmaceutical Chemistry, Kyoto Pharmaceutical University, Yamashina-ku, Kyoto 607-8414, Japan. [b]Faculty of Pure and Applied Sciences, University of Tsukuba, 1-1-1 Tennodai, Tsukuba, Ibaraki 307-8571, Japan. E-mail: furuta@mb.kyoto-phu.ac.jp

This paper is dedicated to Professor Toshiyuki Kan who passed away July 24, 2021.

Abstract – An amide-functionalized thia[7]helicene-like molecule was prepared in an optically active form through the cyclization of the corresponding axially chiral δ-amino acid. X-Ray analysis revealed its twisted helical structure with clockwise helicity and a pairwise association through hydrogen-bonding interactions. This pairwise complex accumulated in the columnar packing in the solid state.

Supramolecular assembly of organic molecules in the solid state has attracted attention in the material sciences for providing special properties and functionalities.[1] Among a variety of molecular assemblies, tubular as well as columnar aggregations formed by helicene and helicene-like molecules through π-π interactions enable special molecular arrangements with unique chiroptical properties.[2]

We have reported the columnar packing of racemic amide-functionalized [7]helicene-like molecule **1** in the single crystal (Figure 1).[3] In this molecular aggregation, the amide functional group modified at the periphery of the fused-ring system works as a molecular recognition site through hydrogen-bonding interaction (Figure 1B). This interaction manifests in a pairwise association between the (*P*)- and (*M*)-enantiomers. The paired complex constructs contain alternating aligned *M*, *P*, *M*, *P* columnar packs, in which the homochiral helicene-like molecules are associated through π-π interactions in each column (Figures 1C).

With the potential for molecular aggregation of helically chiral molecules in mind, it is worth investigating whether columnar aggregation is a typical feature of this series of amide-functionalized helicene-like

molecules. Whether columnar aggregation is a feature specific to racemic (heterochiral) helicene-like molecules such as (*dl*)-**1** or if it can also be formed by enantiopure (homochiral) helicene-like molecules is also of interest.

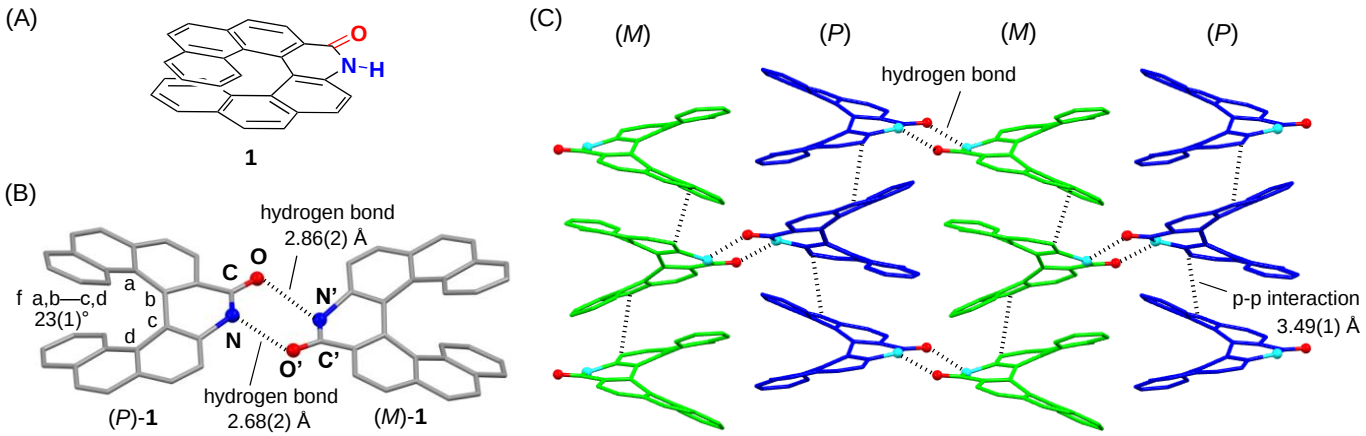

Figure 1. (A) Structure of **1**. (B) Association of (*P*)-**1** and (*M*)-**1** in the single crystal of (*dl*)-**1**. (C) Columnar packing of (*dl*)-**1**.

During the course of our investigation on developing an axially chiral *δ*-amino acid bearing the aniline-type amine and carboxy groups,[4] sulfur-containing axially chiral *δ*-amino acid (*S*)-**2** was prepared and found to be cyclized into the corresponding optically active amide-functionalized thia[7]helicene-like molecule (*P*)-**3** (Figure 2). This finding became the motivation for us to approach the above questions regarding molecular aggregations. Furthermore, synthetic as well as structural interests in thiahelicenes and thiahelicene-like molecules led us to investigate the structural and chiroptical properties of (*P*)-**3**. Herein, we report the synthesis of (*P*)-**3** and its stereostructure, as well as its molecular aggregation as a single crystal.

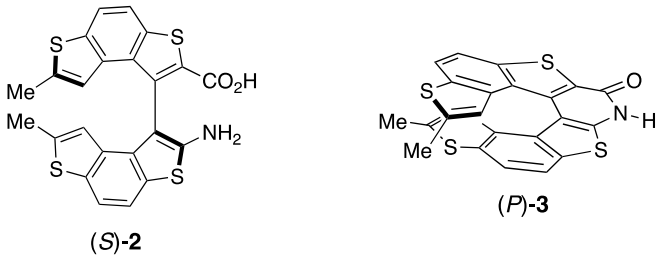

Figure 2. Structures of (*S*)-**2** and (*P*)-**3**

We began the synthesis from the selective monohydrolysis of biaryl diester (*S*,*S*,*S*)-**4**, reported by Tanaka and Osuga,[5] to discriminate the alkoxycarbonyl groups. The reaction conditions are depicted in Table 1.

With treatment of bases (Na_2CO_3, K_2CO_3, and Cs_2CO_3) in the mixed solvent system (THF/H_2O) for 24 h, the desired monoester (*S*)-**5** was obtained; however, the yields were unsatisfactory (Entries 1–3). With replacement of the base into NaOH, the hydrolysis proceeded rapidly to give (*S*)-**5** within 30 min, although the yield remained low (Entry 6). Therefore, LiOH was employed in Entries 4 and 5. Although the yield was still disappointing with regards to the longer reaction time due to significant formation of the corresponding dicarboxylic acid (Entry 5), the yield was increased using a shorter reaction time (0.4 h) and afforded (*S*)-**5** in 69% yield (Entry 4). This relatively rapid hydrolysis might suggest high reactivities of the ester moieties of **4**. Therefore, the use of milder basic LiOH than NaOH and the shorter reaction time are important for selective cleavage of the ester moiety. Thus, selective monohydrolysis was achieved with a reasonable yield.

Table 1. Selective hydrolysis of (*S*,*S*,*S*)-**4** to (*S*)-**5**

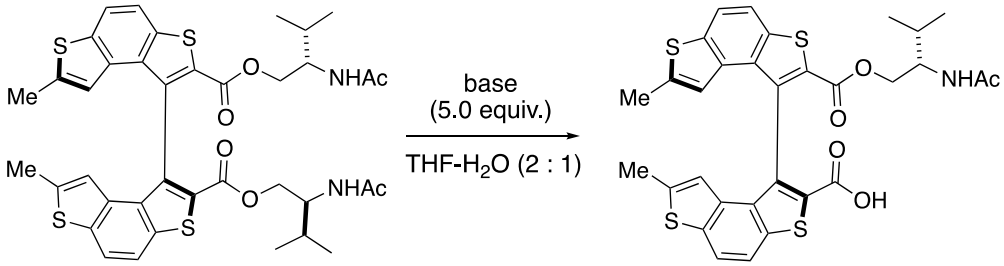

(*S*,*S*,*S*)-**4** (*S*)-**5**

Entry	Base	Time (h)	Yield (%)[a]
1	Na_2CO_3	24	30
2	K_2CO_3	24	23
3	Cs_2CO_3	24	37
4	LiOH	0.4	69
5	LiOH	1.3	10
6	NaOH	0.4	26

[a]Isolated yield.

With a sufficient amount of monoester (*S*)-**5** in hand, we then focused on the transformation to axially chiral *δ*-amino acid (*S*)-**2** (Scheme 1). Curtius rearrangement of (*S*)-**5** in the presence of *t*-BuOH yielded *N*-Boc-protected ester (*S*)-**6**. Deprotection of the Boc group and hydrolytic cleavage of the ester moiety afforded axially chiral *δ*-amino acid (*S*)-**2**.[6] During the chemical transformation of (*S*)-**2**, the conditions yielded the amide-functionalized thia[7]helicene-like molecule (*P*)-**3**.[7] Upon treatment of (*S*)-**2** with TFAA in the presence of DIPEA at room temperature, the lactamization proceeded smoothly to give (*P*)-**3** in 80% yield.[8]

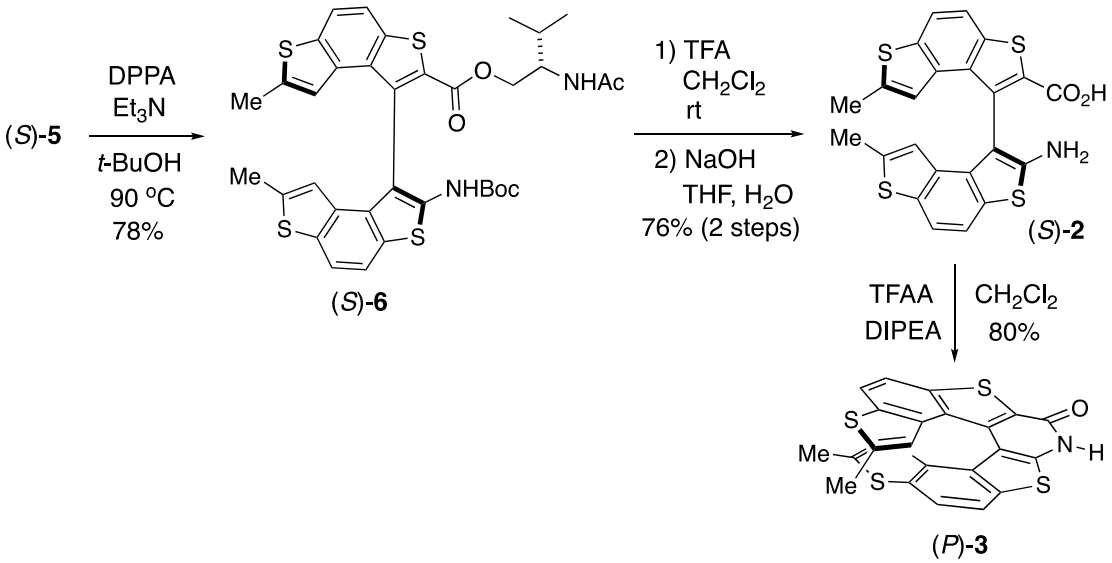

Scheme 1. Transformation to (*P*)-**3** via axially chiral *δ*-amino acid (*S*)-**2**

To reveal the stereostructure and the molecular aggregation of **3** in the solid state, X-ray analysis of its single crystal was examined. It was revealed that (*P*)-**3** possesses a typical helicene-like structure with a clockwise helicity (Figure 3A, ϕa,b–c,d: 19(3)°).[9] As expected, the amide group worked as a hydrogen-bonding site that caused the self-association of (*P*)-**3** (O···N' = 2.84(3) Å; O'···N = 2.71(3) Å) in the crystal. This hydrogen-bonded pair formed a columnar aggregation as shown in Figure 3C. Taking the columnar aggregation of (*dl*)-**1** into account (Figure 1C), formation of the hydrogen-bonding pair and its columnar aggregation in their single crystals might be a common feature of this type of amide-functionalized [7]helicene-like molecule regardless of homochiral (optically pure) or heterochiral (racemic) mixtures. This aggregation could arise from the structural feature of amide-functionalized helical molecules that include two molecular recognizable moieties—the amide and the twisted wide π-system—in which the former causes molecular aggregation toward a horizontal direction through hydrogen-bonding interactions and the latter guides the molecular assembly toward a vertical direction through π-π interactions. The difference between the aggregation of (*dl*)-**1** and (*P*)-**3** is the direction of the hydrogen-bonding interactions which connect each column. In the case of (*P*)-**3**, the hydrogen-bonding interactions connecting each column spread in four directions (Figure 4A), although the hydrogen-bonding interactions connecting the homochiral columns of (*dl*)-**1** were extended into two directions (Figure 4B).[3]

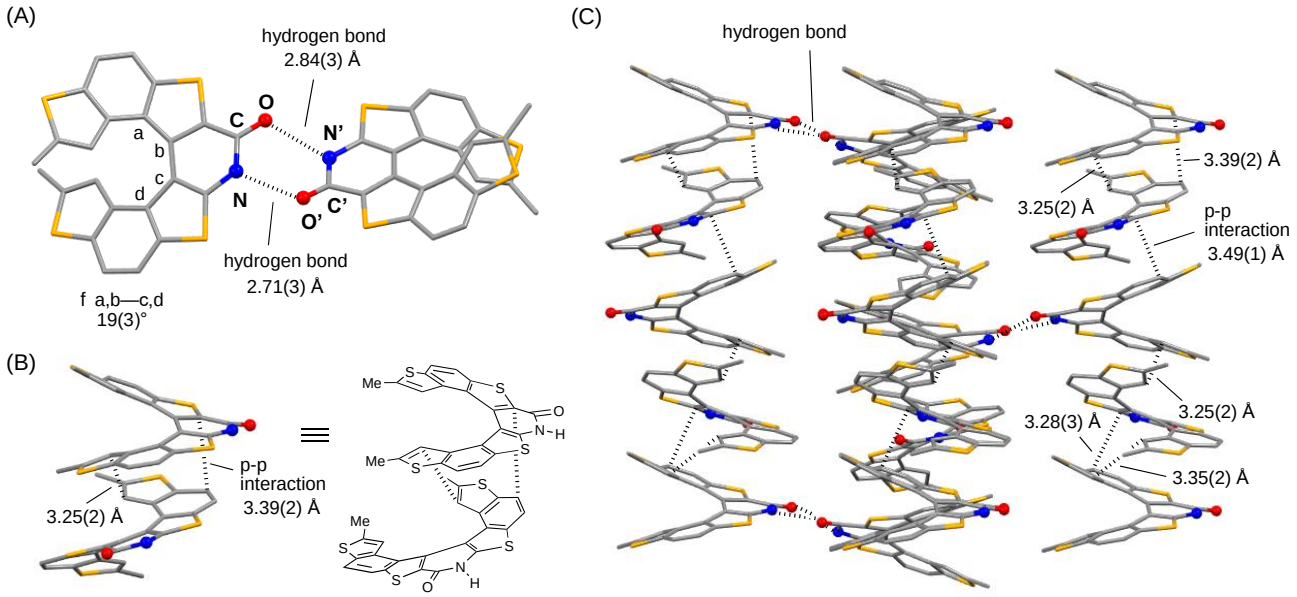

Figure 3. Crystal structure of (*P*)-**3**. Hydrogen atoms are omitted for clarity. (A) Association of (*P*)-**3** via hydrogen-bonding interactions. (B) Typical distances of π-π stacking interactions in a homochiral column of (*P*)-**3**. (C) Columnar packing of (*P*)-**3** in the single crystal.

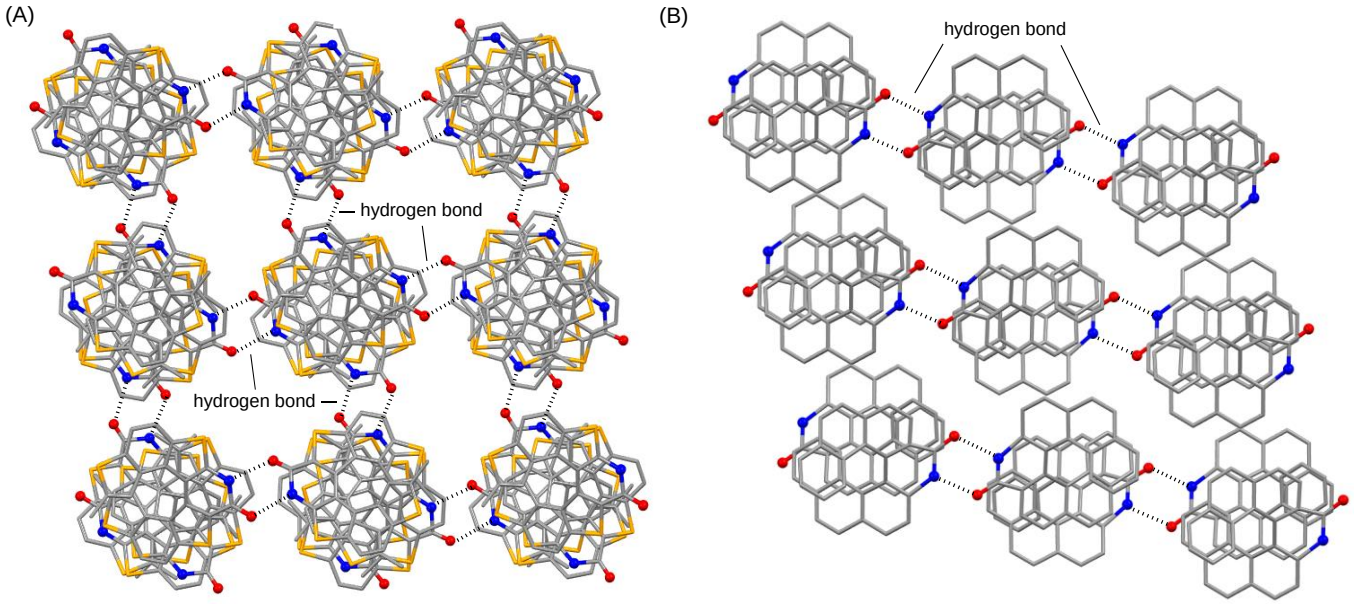

Figure 4. (A) View of columnar aggregation of (*P*)-**3**. (B) View of columnar aggregation of (*dl*)-**1**.

The aggregative property of (*P*)-**3** could be attractive for further applications in material sciences and chiral chemistry, if (*P*)-**3** has abundant configurational stability. Therefore, the configurational stability of **3** was investigated. We have confirmed that **1** has a sufficiently high racemization barrier ($\Delta G^{\ddagger}$ = 41.4 kcal/mol) to be configurationally stable at ambient temperature by DFT calculation.[3] In this case, the racemization barrier of **3** was also examined by DFT calculation and was estimated to be 38.8 kcal/mol at the *ω*B97xd/6-311+G(d,p)//B3LYP/6-31G(d,p) level, in theory, using chlorobenzene as the solvent (Figure 5).[10] This

calculation indicated that (*P*)-**3** also possesses sufficient configurational stability, although its racemization barrier was suggested to be lower than that of **1**. The calculation revealed that the racemization proceeds through a C_s-symmetric transition state structure, which also appears in the case of the racemization of **1**.[3,11]

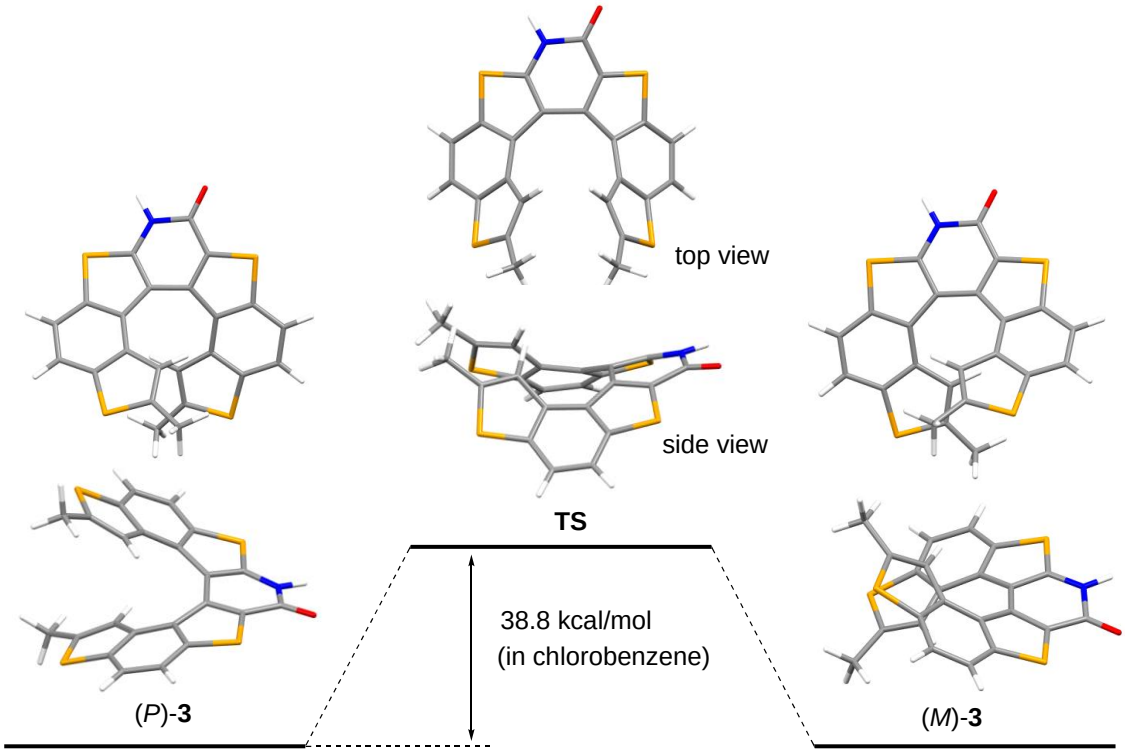

Figure 5. Racemization barrier of **3** and its optimized ground state and transition state structures deduced by DFT calculations

Furthermore, the relatively high optical rotation of (*P*)-**3** ($[\alpha]_D^{20}$ +1559.6)[12] and apparent CD spectrum showed positive Cotton effects from 320 nm to 370 nm and from 235 nm to 310 nm, suggesting its potential as a chiral element for optical devices (Figure 6). In addition, the electronic property of (*P*)-**3** was investigated by DFT calculation at B3LYP/6-31G(d,p) level of theory (Figure 7). Both of the HOMO and LUMO were found to be localized in the pyridone moiety. This is consistent with no absorption maxima in the wavelength longer than 440 nm in the UV-vis absorption spectrum of (*P*)-**3** (Figure 6).

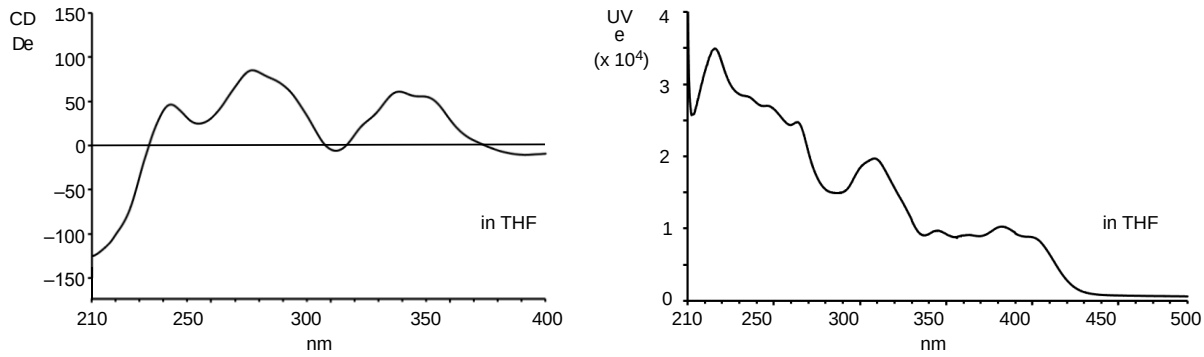

Figure 6. CD and UV spectra of (*P*)-**3** in THF

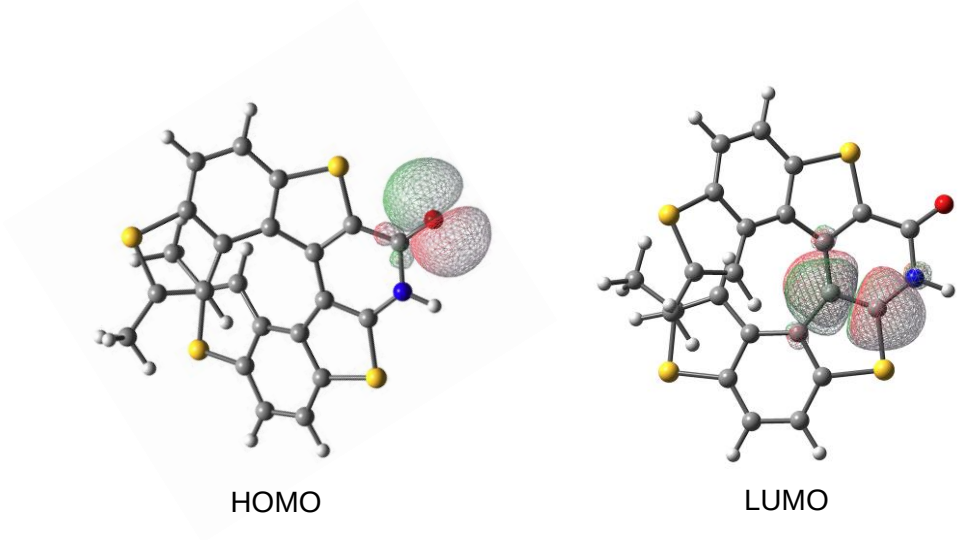

Figure 7. HOMO and LUMO of (*P*)-**3** obtained by DFT calculation at B3LYP/6-31G(d,p) level of theory

In conclusion, we have prepared an amide-functionalized thia[7]helicene-like molecule through the cyclization of the corresponding axially chiral *d*-amino acid. X-Ray analysis revealed its columnar aggregation, which might be a common property of this type of amide-functionalized helical molecule. Further investigation on the molecular assembly of amide-functionalized helical molecules by preparing related derivatives is currently in progress in our laboratory.

EXPERIMENTAL

General Methods

NMR spectra were obtained with a Bruker Ascend 500 spectrometer with chemical shifts in ppm (^{1}H NMR in $CDCl_3$: $CHCl_3$ as internal standards, indicating 7.26; tetramethylsilane as internal standards, indicating 0; ^{13}C NMR in $CDCl_3$: $CDCl_3$ as internal standards, indicating 77.0. ^{1}H NMR in acetone-d_6: acetone as internal standards, indicating 2.04; ^{13}C NMR in acetone-d_6: acetone-d_6 as internal standards, indicating

206.5. ^{1}H NMR in CD_3OD: methanol as internal standards, indicating 3.30; ^{13}C NMR in CD_3OD: methanol as internal standards, indicating 49.0. Spin-spin coupling constants are in Hz. IR spectra were recorded with a JASCO FT-IR4200 spectrometer. HRMS was recorded with a JEOL JMC-GCmateII or a JEOL MStation JMS-700 spectrometer. Silica gel column chromatography was carried out by using Silica gel 60 N (spherical, neutral, 63~210 μm, Kanto Chemical Co., Inc.). TLC analysis was performed on commercial glass plates bearing a 0.25 mm layer of Merck Kiesel gel 60 F254. All chemicals and reagents were commercially purchased and used without further purification.

Synthetic Procedures

(*S*)-2'-((2-Acetamido-3-methylbutoxy)carbonyl)-7,7'-dimethyl-[1,1'-bibenzo[1,2-*b*:4,3-*b*']dithiophene]-2-carboxylic acid ((*S*)-**5**):

To a solution of (*S*,*S*,*S*)-**4**[5] (312 mg, 0.42 mmol) in THF/H_2O (2/1, 10 mL) was added LiOH•H_2O (87 mg, 2.1 mmol) at rt. After being stirred for 25 min at rt, the reaction was quenched with 2 *N* aq. HCl, and extracted with AcOEt. The organic layer was washed with brine, dried over Na_2SO_4, filtered, and concentrated *in vacuo* to give a residue. The residue was purified by column chromatography (SiO_2, $CHCl_3$/MeOH = 30/1 to 20/1) to give (*S*)-**5** (178 mg, 69%).

Colorless amorphous; $[\alpha]_D^{20}$ –257.6 (c 0.3, $CHCl_3$).; ^{1}H NMR (500 MHz, acetone-d_6) δ 0.52 (3H, d, J = 6.7 Hz), 0.62 (3H, d, J = 6.7 Hz), 0.75–0.85 (1H, m), 1.84 (3H, s), 2.21–2.35 (6H, m), 3.51–3.55 (1H, m), 3.90–4.20 (2H, m), 5.89 (1H, s), 5.97 (1H, s), 6.00–6.10 (1H, m), 8.02 (2H, s), 8.07 (2H, s); ^{13}C NMR (125 MHz, acetone-d_6) δ 16.4, 19.0, 19.6, 23.2, 53.6, 53.7, 66.4, 119.3, 119.4, 120.0, 120.1, 123.2, 123.3, 130.6, 134.2, 134.5, 137.0, 138.6, 138.9, 139.0, 139.1, 139.5, 143.6, 143.8, 163.2, 163.7, 170.1; IR (neat) 2961, 2919, 1694, 1486, 1371, 1258, 1226, 1081, 1024, 793 cm^{-1}; HRMS (FAB): *m/z* calcd for $C_{31}H_{26}NO_5S_4$ $[M–H]^-$ 620.0694, found 620.0699.

(*S*)-2-Acetamido-3-methylbutyl-2'-((*tert*-butoxycarbonyl)amino)-7,7'-dimethyl-[1,1'-bibenzo[1,2-*b*:4,3-*b*']dithiophene]-2-carboxylate ((*S*)-**6**):

To a solution of (*S*)-**5** (165 mg, 0.27 mmol) in *t*-BuOH (15 mL) were added DPPA (114 μL, 0.53 mmol) and Et_3N (0.11 mL, 0.80 mmol) at rt under N_2 atmosphere. After being stirred for 48 h at 90 ℃, the reaction mixture was quenched with sat. aq. NH_4Cl, and extracted with AcOEt. The organic layer was washed with brine, dried over Na_2SO_4, filtered, and concentrated *in vacuo* to give a residue. The residue was purified by column chromatography (SiO_2, *n*-hexane/AcOEt = 5/1 to 1/1) to give (*S*)-**6** (143 mg, 78%).

Yellow amorphous; $[\alpha]_D^{20}$ –303.0 (c 1.0, $CHCl_3$); ^{1}H NMR (500 MHz, $CDCl_3$) δ –0.39–0.37 (1H, m), 0.14 (3H, d, J = 6.6 Hz), 0.39 (3H, d, J = 6.6 Hz), 1.45 (9H, s), 1.95 (3H, s), 2.29 (3H, s), 2.34 (3H, s), 3.35–3.48 (1H, m), 3.96 (1H, dd, J = 11.5 Hz, 2.4 Hz), 4.24 (1H, dd, J = 11.5 Hz, 2.4 Hz), 4.78 (1H, d, J = 9.2 Hz), 5.90 (1H, s), 6.10 (1H, s), 6.60 (1H, s), 7.65–7.75 (2H, m), 7.82–7.95 (2H, m); ^{13}C NMR (125 MHz,

$CDCl_3$) δ 16.3, 16.5, 18.2, 19.9, 23.1, 27.4, 28.1, 53.1, 66.6, 82.9, 113.5, 117.3, 117.8, 118.0, 118.5, 119.0, 122.4, 129.7, 131.2, 132.8, 133.1, 133.3, 134.0, 136.1, 136.2, 137.9, 138.0, 138.9, 141.3, 143.3, 152.2, 163.3, 169.9; IR (neat) 3400, 2964, 2916, 2867, 1696, 1661, 1585, 1507, 1445, 1367, 1275, 1246, 1227, 1151, 1104, 1065, 757 cm^{-1}; HRMS (FAB): *m/z* calcd for $C_{35}H_{35}NO_5S_4$ $[M–H]^-$ 691.1429, found 691.1423.

(*S*)-2'-Amino-7,7'-dimethyl-[1,1'-bibenzo[1,2-*b*:4,3-*b*']dithiophene]-2-carboxylic acid ((*S*)-**2**):

To a solution of (*S*)-**6** (88 mg, 0.13 mmol) in CH_2Cl_2 (6.0 mL) was added trifluoroacetic acid (4.0 mL) at rt. After being stirred for 5 h at rt, the solution was evaporated to give a residue. The residue was dissolved with AcOEt, and washed with sat. aq. $NaHCO_3$ and brine, dried over Na_2SO_4, filtered, and concentrated *in vacuo* to give a residue. The residue was dissolved in THF/H_2O (2/1, 9.0 mL), then 2 *N* aq. NaOH (1.0 mL) was added at rt. After being stirred for 22 h at 50 ℃, the reaction was quenched with 2 *N* aq. HCl, and extracted with AcOEt. The organic layer was washed with water and brine, dried over Na_2SO_4, filtered, and concentrated *in vacuo* to give a residue. The residue was purified by column chromatography (SiO_2, $CHCl_3$/MeOH = 20/1) to give (*S*)-**2** (45 mg, 76%).

Yellow solid; Mp 183–185 ℃; $[\alpha]_D^{20}$ –42.5 (c 0.2, MeOH); ^{1}H NMR (500 MHz, CD_3OD) δ 2.21 (3H, d, *J* = 1.2 Hz), 2.32 (3H, d, *J* = 1.2 Hz), 5.82–5.85 (1H, m), 6.44–6.46 (1H, m), 7.47 (1H, d, *J* = 8.5 Hz), 7.58 (1H, d, *J* = 8.5 Hz), 7.85–7.94 (2H, m); ^{13}C NMR (125 MHz, CD_3OD) δ 15.8, 16.0, 79.5, 108.5, 116.0, 118.5, 118.9, 119.8, 120.9, 122.8, 128.2, 133.2, 134.2, 135.5, 137.7, 138.3, 138.9, 139.5, 140.1, 143.0, 150.3, 165.5; IR (KBr): 3453, 3324, 2920, 2849, 1683, 1656, 1495, 1441, 1407, 1298, 1275, 749 cm^{-1}; HRMS (EI^+): *m/z* calcd for $C_{23}H_{15}NO_2S_4$ $[M]^+$ 464.9986, found 464.9988.

Amide-functionalized thia[7]helicene-like molecule (*P*)-**3**:

To a solution of (*S*)-**2** (88 mg, 0.13 mmol) in CH_2Cl_2 (5 mL) were added DIPEA (67 μL, 384 mmol) and stirred for 5 min. The reaction was warmed and TFAA (33 μL, 0.24 mmol) was added during reflux. After being refluxed for 1 h, the reaction was quenched with sat. aq. NH_4Cl, and extracted with $CHCl_3$. The organic layer was washed with brine, dried over Na_2SO_4, filtered, and concentrated *in vacuo* to give a residue. The residue was purified by recrystallization from *n*-hexane/$CHCl_3$ to give (*P*)-**3** (27 mg, 80%).

Yellow needle; Mp 273–285 ℃ (decomp.); $[\alpha]_D^{20}$ +1559.6 (c 0.2, $CHCl_3$); ^{1}H NMR (500 MHz, $CDCl_3$) δ 2.15 (3H, s), 2.18 (3H, s), 6.50 (1H, s), 6.66 (1H, s), 7.76 (1H, d, *J* = 8.5 Hz), 7.82 (1H, d, *J* = 8.5 Hz), 7.89 (1H, d, *J* = 8.5 Hz), 7.98 (1H, d, *J* = 8.5 Hz), 12.50 (1H, br s); ^{13}C NMR (125 MHz, $CDCl_3$) δ 15.60, 15.64, 113.4, 117.5, 118.0, 119.2, 122.8, 123.4, 124.2, 127.9, 128.9, 129.6, 129.8, 135.6, 136.7, 137.3, 137.9, 138.8, 140.1, 140.7, 143.4, 160.0; IR (KBr): 2644, 1615, 1123, 751, 567 cm^{-1}; CD λ_{ext} (THF) nm ($\Delta\varepsilon$): 339 (60.78), 312 (–5.93), 277 (84.96), 243 (46.20); UV λ_{max} (THF) nm (log ε): 396 (4.00), 319 (4.29), 274 (4.39), 226 (4.54)； HRMS (EI^+): *m/z* calcd for $C_{23}H_{13}NOS_4$ $[M]^+$ 446.9880, found 446.9879.

Crystallographic data for the single crystal of (*P*)-**3** obtained by recrystallization from $CHCl_3$ and *n*-hexane: $C_{23}H_{13}NOS_4$, M = 447.58, orthorhombic, $P2_12_12_1$, a = 14.6449(3), b = 16.0013(3), c = 19.6150(4) Å, α = 90°, β = 90°, γ = 90°, V = 4596.53(16) $Å^3$, Z = 4, ρ_{calcd} = 1.294 gcm^{-3}, T = 103 K, 51019 reflections measured, 8530 unique. The final R_1 and wR were 0.0738 and 0.1927 (all data). These data have been deposited with the Cambridge Crystallographic Data Center as CCDC 2124393.

ACKNOWLEDGEMENTS

This work was financially supported by a Grant-in-Aid for Scientific Research (B) (18H02554).

REFERENCES AND NOTES

1. For reviews, see: a) V. A. Russell and M. D. Ward, *Chem. Mater.*, 1996, **8**, 1654; b) J. D. Wuest, *Chem. Commun.*, 2005, 5830; c) N. B. McKeown, *J. Mater. Chem.*, 2010, **20**, 10588; d) G. R. Desiraju, *J. Am. Chem. Soc.*, 2013, **135**, 9952.
2. For examples of tubular and columnar organization of helicene and heterohelicenes, see: a) T. Verbiest, S. V. Elshocht, M. Kauranen, L. Hellemans, J. Snauwaert, C. Nuckolls, T. J. Katz, and A. Persoons, *Science*, 1998, **282**, 913; b) B. Busson, M. Kauranen, C. Nuckolls, T. J. Katz, and A. Persoons, *Phys. Rev. Lett.*, 2000, **84**, 79; c) T. Verbiest, S. V. Elshocht, A. Persoons, C. Nuckolls, K. E. Phillips, and T. J. Katz, *Langmuir*, 2001, **17**, 4685; d) K. E. S. Phillips, T. J. Katz, S. Jockush, A. J. Lovinger, and N. J. Turro, *J. Am. Chem. Soc.*, 2001, **123**, 11899; e) K. Nakano, Y. Hidehira, K. Takahashi, T. Hiyama, and K. Nozaki, *Angew. Chem. Int. Ed.*, 2005, **44**, 7136; f) M. A. Shcherbina, X.-B. Zeng, T. Tadjiev, G. Ungar, S. H. Eichhorn, K. E. S. Phillips, and T. J. Katz, *Angew. Chem. Int. Ed.*, 2009, **48**, 7837; g) V. Terrasson, M. Roy, S. Moutard, M.-P. Lafontaine, G. Pépe, G. Félix, and M. Gingras, *RSC Adv.*, 2014, **4**, 32412; h) K. Usui, K. Yamamoto, Y. Ueno, K. Igawa, R. Hagihara, T. Masuda, A. Ojida, S. Karasawa, K. Tomooka, G. Hirai, and H. Suemune, *Chem. Eur. J.*, 2018, **24**, 14617; i) T. Hirao, Y. Ono, N. Kawata, and T. Haino, *Org. Lett.*, 2020, **22**, 5294; j) S. Kinoshita, R. Yamano, Y. Shibata, Y. Tanaka, K. Hanada, T. Matsumoto, K. Miyamoto, A. Muranaka, M. Uchiyama, and K. Tanaka, *Angew. Chem. Int. Ed.*, 2020, **59**, 11020.
3. Y. Xing, M. Nikaido, T. Murai, S. Hamada, Y. Kobayshi, T. Sasamori, T. Kawabata, and T. Furuta, *Heterocycles*, 2021, **103**, 544.
4. a) T. Furuta, J. Yamamoto, Y. Kitamura, A. Hashimoto, H. Masu, I. Azumaya, T. Kan, and T. Kawabata, *J. Org. Chem.*, 2010, **75**, 7010; b) T. Furuta, M. Nikaido, J. Yamamoto, T. Kuribayashi, and T. Kawabata, *Synthesis*, 2013, **45**, 1312; c) T. Murai, Y. Xing, T. Kuribayashi, W. Lu, J.-D. Guo, R. Yella, S. Hamada, T. Sasamori, N. Tokitoh, T. Kawabata, and T. Furuta, *Chem. Pharm. Bull.*, 2018, **66**, 1203; d) S. Hamada, S. Wang, T. Murai, Y. Xing, T. Inoue, Y. Ueda, T. Sasamori, T. Kawabata,

and T. Furuta, *Heterocycles*, 2020, **101**, 328.

5. K. Tanaka, H. Suzuki, and H. Osuga, *J. Org. Chem.*, 1997, **62**, 4465.
6. (*S*)-**2** was found to be stable and storable without forming (*P*)-**3**.
7. Reviews on thiahelicene and thiahelicene-like molecules, see: a) S. K. Collins and M. P. Vachon, *Org. Biomol. Chem.*, 2006, **4**, 2518; b) Y. Shen and C.-F. Chen, *Chem. Rev.*, 2012, **112**, 1463. See also Ref. 6, and c) M. Shyam and A. V. Bedekar, *Org. Lett.*, 2015, **17**, 5808; d) T. Yanagi, T. Tanaka, and H. Yorimitsu, *Chem. Sci.*, 2021, **12**, 2784.
8. The absolute configuration of (*P*)-**3** was determined by the X-ray analysis as shown in Figure 3.
9. The crystal structure of (*P*)-**3** is disordered over two positions; only one of the disordered structures is shown in Figure 3. For the full disordered structures, see the Supporting Information. The X-ray data for (*P*)-**3** has been deposited at the Cambridge Crystallographic Data Center under reference number CCDC 2124393.
10. For computational details, see the Supporting Information.
11. Following reference discussed about *C*s-symmetric transition state for racemization, see, a) R. H. Janke, G. Haufe, E.-U. Würthwein, and J. H. Borkent, *J. Am. Chem. Soc.*, 1996, **118**, 6031; b) J. Barroso, J. L. Cabellos, S. Pan, F. Murillo, X. Zarate, M. A. Fernandez-Herrera, and G. Merino, *Chem. Commun.*, 2018, **54**, 188.
12. The specific rotation of (*P*)-**3** was found to be smaller than that of corresponding thia[7]helicene (*P*)-**7** (($[\alpha]_D$ +2720 (c 0.0557, $CHCl_3$)). See, Ref. 5.

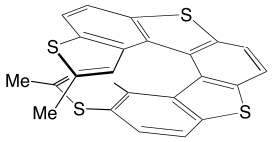

(*P*)-**7**